ELECTRON MOTION IN SOLENOIDAL MAGNETIC FIELDS USING A FIRST-ORDER SYMPLECTIC INTEGRATION ALGORITHM*

J. S. Fraser, Group AT-7, MS-H825
Los Alamos National Laboratory, Los Alamos, New Mexico 87544 USA

Summary

The use of nonsymplectic procedures in particle tracing codes for relativistic electrons leads to errors that can be reduced only at the expense of using very small integration steps. More accurate results are obtained with symplectic transformations for position and momentum. A first-order symplectic integration procedure requires an iterative calculation of the new position coordinates using the old momenta, but the process usually converges in three or four steps. A first-order symplectic algorithm has been coded for cylindrical as well as Cartesian coordinates using the relativistic equations of motion with Hamiltonian variables. The procedure is applied to the steering of a beam of 80-keV electrons by a weak transverse magnetic field superposed on a strong magnetic field in the axial direction. The steering motion is shown to be parallel to the transverse field rather than perpendicular as would be the case without the strong axial field.

Introduction

In a typical high-current electron injector for a linac, a solenoidal focusing field is required to transport the beam through the buncher drift space. To aim the beam precisely on the linac axis, a weak-steering magnetic field can be superposed orthogonally to the focusing field. The electron motion is complicated in the combined fields. Initial attempts at numerical integration of the electron's equations of motion using a simple, nonsymplectic transformation revealed large errors in position and momentum. A high-order Runge-Kutta numerical integration procedure can be used, but the number of function evaluations per step is large.

An alternative approach, based on a symplectic integration algorithm[1-3] achieves an accurate result with a modest number of function evaluations per step. The relativistic Hamiltonian for a particle in a static magnetic field is used with Hamilton's equations of motion. The resulting integration procedure is applied to studying the steering of an 80-keV electron beam in a combined strong axial and weak radial magnetic field.

First-Order Symplectic Transformation

At each integration step, with time as the independent variable, the canonical variables q and p are advanced in the time interval h according to the transformations $q = q_0 + h\dot{q}$, and $p = p_0 + h\dot{p}$. Channell[2] has shown that the lowest order symplectic transformation is given by the equations of motion

$$\dot{q} = \frac{\partial H}{\partial p_0}(q,p_0) \quad , \text{ and}$$

$$\dot{p} = -\frac{\partial H}{\partial q}(q,p_0) \quad ,$$

where the Hamiltonian is a function of the new position variables q and the old momentum variables p_0.

The q transformation is an implicit function of q that must be evaluated by iteration using the old momentum p_0. Following the iteration, the force term is evaluated at the new position with the old momentum. Intrinsic properties of the symplectic transformation are the conservation of energy and the fact that the determinant of its Jacobian matrix is unity,[1,4] implying that Liouville's theorem is satisfied. A nonsymplectic transformation results if q is replaced by q_0 in the equations of motion.

For motion in a static magnetic field, the relativistic Hamiltonian

$$H = \gamma m_0 c^2 = \left[m_0^2 c^4 + c^2(\bar{p} - e\bar{A})^2\right]^{1/2}$$

gives the following set of symplectic transformations for canonical variables in Cartesian coordinates:

$$x = x_0 + \frac{h}{\gamma m_0}(p_{x0} - eA_x) \quad , \tag{1}$$

$$y = y_0 + \frac{h}{\gamma m_0}(p_{y0} - eA_y) \quad , \tag{2}$$

$$z = z_0 + \frac{h}{\gamma m_0}(p_{z0} - eA_z) \quad , \tag{3}$$

$$p_x = p_{x0} + \frac{he}{\gamma m_0}\left[(p_{x0} - eA_x)\frac{\partial A_x}{\partial x} + (p_{y0} - eA_y)\frac{\partial A_y}{\partial x} + (p_{z0} - eA_z)\frac{\partial A_z}{\partial x}\right] \quad , \tag{4}$$

$$p_y = p_{y0} + \frac{he}{\gamma m_0}\left[(p_{x0} - eA_x)\frac{\partial A_x}{\partial y} + (p_{y0} - eA_y)\frac{\partial A_y}{\partial y} + (p_{z0} - eA_z)\frac{\partial A_z}{\partial y}\right] \quad , \text{ and} \tag{5}$$

$$p_z = p_{z0} + \frac{he}{\gamma M_0}\left[(p_{x0} - eA_x)\frac{\partial A_x}{\partial z} + (p_{y0} - eA_y)\frac{\partial A_y}{\partial z} + (p_{z0} - eA_z)\frac{\partial A_z}{\partial z}\right] \quad , \tag{6}$$

where it is understood that A_q = is the q component of the vector potential A(x,y,z). The (p - eA) terms are the mechanical momenta. For eqs. (1) to (6), the value of the determinant for the Jacobian matrix of the transformations was found to be one to within the round-off error of the computer.

Electron Motion in Complex Magnetic Fields

The steering problem discussed in the introduction can be simulated accurately by superposing magnetic fields and vector potentials produced by orthogonal arrays of circular coils. A code was written to integrate the equations of motion using the symplectic transformations of the previous section. The subroutines that computed the magnetic-field and vector-potential components and the nine partial derivatives in eqs. (4) to (6) were checked numerically to ensure that $\nabla \cdot A = 0$ and that the magnetic-field components were consistent with $B = \nabla \times A$. Space-charge forces were ignored.

*Work supported by the US Department of Defense under the auspices of the US Department of Energy.

At each step of the integration, eqs. (1) to (3) are solved by iteration, the vector potentials being evaluated at the new position. An absolute error of not more than 10^{-7} m in position was found to be adequate for a typical problem. The vector potentials and partial derivatives at the new position were then used in eqs. (4) to (6).

Electron Motion in Combined Focusing and Steering Magnetic Fields

Combined focusing and steering magnetic fields such as those used in the 80-keV electron injector of the Los Alamos National Laboratory free electron laser linac are simulated by two orthogonal arrays of circular coils as shown in fig. 1. The longitudinal and transverse fields from such a coil set are illustrated in fig. 2. For an illustrative calculation, a beam of

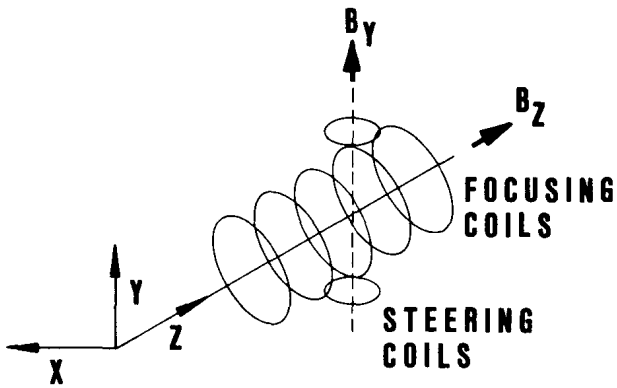

Fig. 1. Schematic diagram of two orthogonal arrays of coils simulating the combined use of focusing and steering magnetic fields.

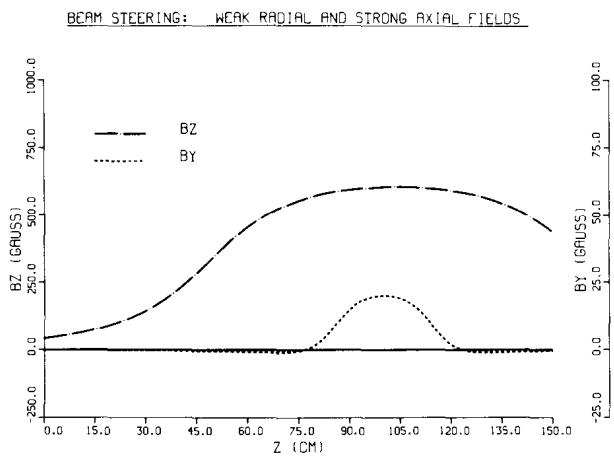

Fig. 2. Longitudinal and transverse magnetic fields from a coil set similar to that of fig. 1.

electrons in a narrow, hollow cone is launched on the z-axis of the focusing field. The position and shape of the beam are shown at six z-locations in fig. 3. It is interesting to note that when the steering field, here in the y-direction, is weak in comparison with the focusing field, the steering of the beam centroid is in the plane of the steering field and not perpendicular to it.

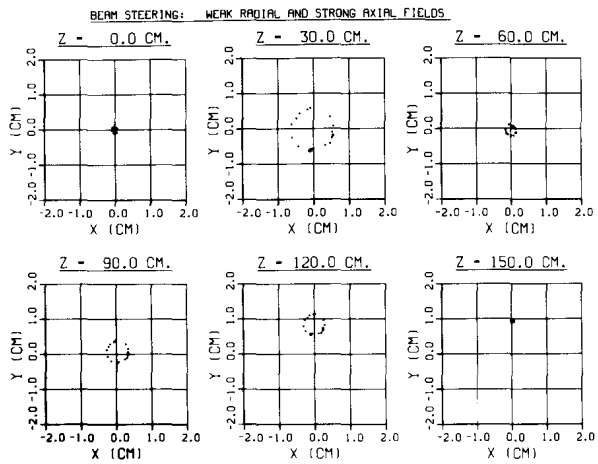

Fig. 3. Transverse beam profiles at six locations in the field of fig. 2 for a hollow cone of 80-keV electrons. The centroid is steered parallel to the steering component field B_y.

Figure 4 shows the transverse coordinates of a single particle and the fractional error in the total momentum. The degree of accuracy in conserving total momentum or energy is a useful criterion of the integration algorithm's accuracy. The fractional momentum error in fig. 4 is cyclic in the fringing-field regions with a maximum value of about 5×10^{-5} for a step size of 10-ps that corresponds to about 76 steps per cyclotron period. The momentum error scales approximately linearly with the step size.

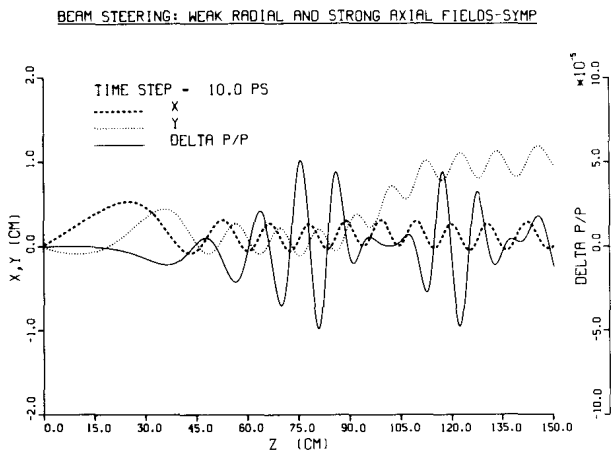

Fig. 4. Transverse coordinates and fractional momentum error for an 80-keV electron in the field of fig. 2.

When a focusing field is not superposed on a steering field (the usual case), the expected result is as shown in fig. 5 for the same steering field given in fig. 3 as B_y. Here the centroid motion is perpendicular to the steering field, and the steering effect is much enhanced. For axial fields between zero and a value large compared with the radial field, the steering direction varies from perpendicular to the radial field to parallel to the radial field.

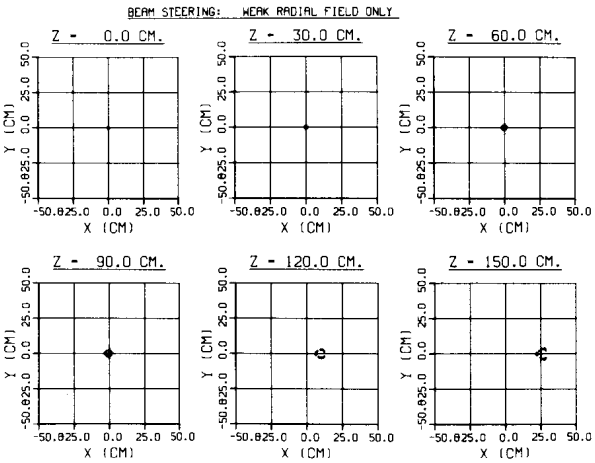

Fig. 5. As in fig. 3, but with only the B_y field component present. The centroid is steered perpendicular to the steering field B_y.

Comparison of Runge-Kutta, Symplectic, and Nonsymplectic Procedures

Electron motion in the combined fields of fig. 2 was computed with a standard fourth-order, adaptive Runge-Kutta procedure, the first-order symplectic transformation of eqs. (1) to (6) and the first-order nonsymplectic transformation that results from evaluating the vector potential at (x_0,y_0,z_0). The result of the nonsymplectic calculation corresponding to the symplectic calculation shown in fig. 4 is given in fig. 6. The momentum error grows monotonically and the transverse motion is unstable. By contrast, the use of the Runge-Kutta routine gives a highly accurate result as shown in fig. 7.

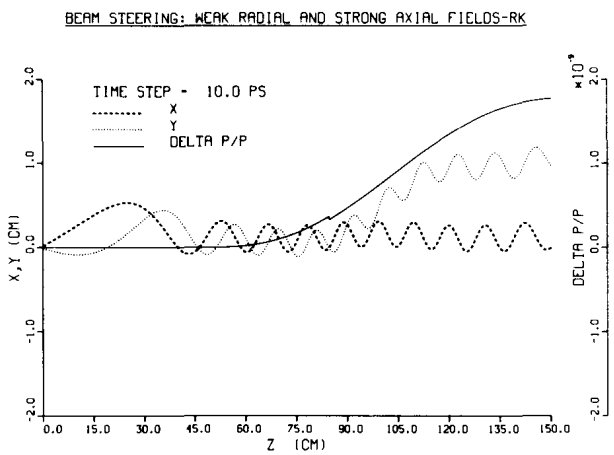

Fig. 6. As in fig. 4, but with integration by a nonsymplectic transformation.

For the field of fig. 2, a summary of the results obtained with the three procedures is given in table I for a range of step sizes. The step size is given in terms of the steps per cyclotron period at the B_z-field maximum where the period is approximately 0.76 ns for 80-keV electrons.

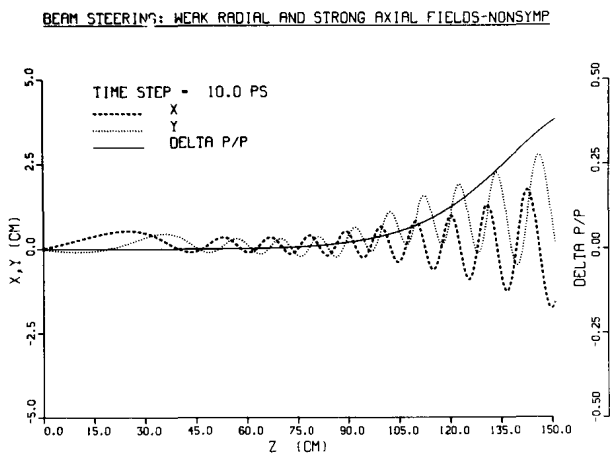

Fig. 7. As in fig. 4 both with integration by a fourth-order Runge-Kutta procedure.

TABLE I

COMPARISON OF RESULTS FROM THREE INTEGRATION PROCEDURES FOR 80-keV ELECTRONS IN THE MAGNETIC FIELD OF FIGURE 2.

	Time Steps Per Cyclotron Period	Function Calls Per Cyclotron Period	Relative CPU Time	Fractional Momentum Error $\Delta p/p$
Fourth-order Runge-Kutta	760	5320	68	1×10^{-11}
	76	547	7	2×10^{-9}
	7.6	304	2.1	1×10^{-8}
First-order symplectic	760	1520	19	5×10^{-6}
	76	290	3.4	5×10^{-5}
	7.6	114	1	5×10^{-4}
First-order nonsymplectic	760	760	11	3×10^{-2}
	76	76	1.3	3×10^{-1}
	7.6	7.6	---	failed

Clearly the Runge-Kutta procedure gives an accurate result even with 7.6 steps per cyclotron period. If a high degree of accuracy is required, this procedure is the preferred one. The first-order symplectic algorithm gives an accuracy acceptable for most purposes with a reduction in computer time. The nonsymplectic algorithm, on the other hand, although economic in function calls per step, is acceptable only for very small time steps.

Conclusions

A first-order symplectic algorithm for integrating the relativistic equations of motion for electrons in complex magnetic-field configurations is more accurate than a nonsymplectic algorithm. Although the fourth-order Runge-Kutta procedure is far more accurate than the symplectic algorithm considered here, the latter is simpler to use and of sufficient accuracy for most beam-transport applications.

References

1. A. J. Dragt, "Lectures on Nonlinear Orbit Dynamics," Physics of High Energy Accelerators, Eds: R. A. Carrigan, F. R. Huson, and M. Month, A.I.P. Conf. Proc. No. 87, 1981, 147.
2. P. J. Channell, "Symplectic Integration Algorithms," Los Alamos National Laboratory internal report, AT-6: ATN-83-9, 1983.
3. R. D. Ruth, "A Canonical Integration Technique," Proc. 1983 Particle Accelerator Conf., Santa Fe, New Mexico, March 21-23, 1983, IEEE Trans. Nucl. Sci. 30, No. 4, 2669 (August 1983).
4. M. Hammermesh, Group Theory And Its Application To Physical Problems (Addison-Wesley, Reading, Massachusetts, 1962), 406.